Journal of King Saud University - Science 36 (2024) 103089

HOSTED BY

Contents lists available at ScienceDirect

Journal of King Saud University - Science

journal homepage: www.sciencedirect.com

Full Length Article

Green synthesis of CuO nanoparticles using *Jasmin sambac* extract: Conditions optimization and photocatalytic degradation of Methylene Blue dye

Shazia Nouren [a], Ismat Bibi [b], Abida Kausar [c], Misbah Sultan [d], Haq Nawaz Bhatti [e], Yusra Safa [f], Sana Sadaf [g], Norah Alwadai [h,*], Munawar Iqbal [i,*]

[a] *Department of Chemistry, Government College Women University, Sialkot, Pakistan*
[b] *Institute of Chemistry, The Islamia University of Bahawalpur, Bahawalpur, Pakistan*
[c] *Department of Chemistry, Government College Women University, Faisalabad, Pakistan*
[d] *School of Chemistry, University of the Punjab, Lahore, Pakistan*
[e] *Department of Chemistry, University of Agriculture, Faisalabad, Pakistan*
[f] *Department of Chemistry, Lahore College for Women University, Lahore, Pakistan*
[g] *Bio-analytical Chemistry Laboratory, Punjab Bio-Energy Institute, University of Agriculture, Faisalabad, Pakistan*
[h] *Department of Physics, College of Sciences, Princess Nourah bint Abdulrahman University, P.O. Box 84428, Riyadh 11671, Saudi Arabia*
[i] *Department of Chemistry, Division of Science and Technology, University of Education, Lahore, Pakistan*

ARTICLE INFO

Keywords:
Green synthesis
CuO nanoparticles
Photocatalysis
Dye degradation

ABSTRACT

This investigation utilized an eco-friendly method to produce copper oxide nanoparticles (CuO NPs) through the utilization of *Jasminium sambac* leaf extract. Optimization of pH, temperature, reaction time, and copper sulfate concentration were performed. Characterization via UV–Vis, SEM, XRD, FTIR, and EDX techniques revealed a peak at 243 nm in UV–Vis, and an FTIR band at 590 cm^{-1} confirmed Cu(II) ion reduction to CuO NPs. pH, temperature, reaction time, and copper sulfate concentration were identified as crucial synthesis parameters. EDX analysis indicated a composition of 75.94% copper and 24.06% oxygen. CuO NPs were dispersive, monoclinic, crystalline, and pure, with an average particle size of 13.4 nm. Photocatalytic experiments achieved 97% Methylene Blue dye degradation in 210 min, highlighting the efficacy of the green synthesis method for CuO NPs with significant photocatalytic activity in wastewater remediation.

1. Introduction

Nanotechnology's impact in recent decades has been significant, especially due to the unique properties of nanoparticles arising from their nanoscale size. With a higher surface-to-volume ratio, nanoparticles find versatile applications across various fields (Alfanaar et al., 2021, Nagesh et al., 2022, Sivakavinesan et al., 2022). In the NP synthesis, a reduction of metal ions is performed using an appropriate reducing agent. In view of the existing situation of environmental contamination (Iqbal et al., 2019). The demand for eco-friendly nanomaterial preparation has grown. Conventional synthesis methods involve hazardous reagents, extended reaction times, and high costs. Green chemistry tackles these challenges by employing economical and environmentally friendly agents. Plant extracts, rich in natural carboxyl and hydroxyl groups, present ideal substitutes for chemicals in environmentally friendly synthesis. They adeptly reduce metal ions to metal atoms at the nano-scale, serving as dual-function agents for both reduction and stabilization (Shammout and Awwad 2021). The *Jasminium sambac* leaves are rich in phenolic compounds and can be used for green synthesis of NP since it is rich in antioxidant activity (Widowati et al., 2018). Green synthesis is more cost-effective and time-efficient than traditional physical and chemical methods for nanoparticle synthesis, requiring no normal energy, pressure, or heating conditions, and avoiding the use of harmful chemicals (Naseer et al., 2020, Amer and Awwad 2021, Shammout and Awwad 2021).

The textile industry contributes significantly to water pollution through the discharge of industrial waste containing colored chemicals. This leads to reduced dissolved oxygen, increased turbidity, and interference with natural photosynthesis in water bodies. The MB dye, commonly used in aquaculture for fish disease treatment and as a mild

* Corresponding authors.
E-mail addresses: nmalwadai@pnu.edu.sa (N. Alwadai), bosalvee@yahoo.com (M. Iqbal).

https://doi.org/10.1016/j.jksus.2024.103089
Received 15 November 2022; Received in revised form 29 December 2023; Accepted 1 January 2024
Available online 2 January 2024

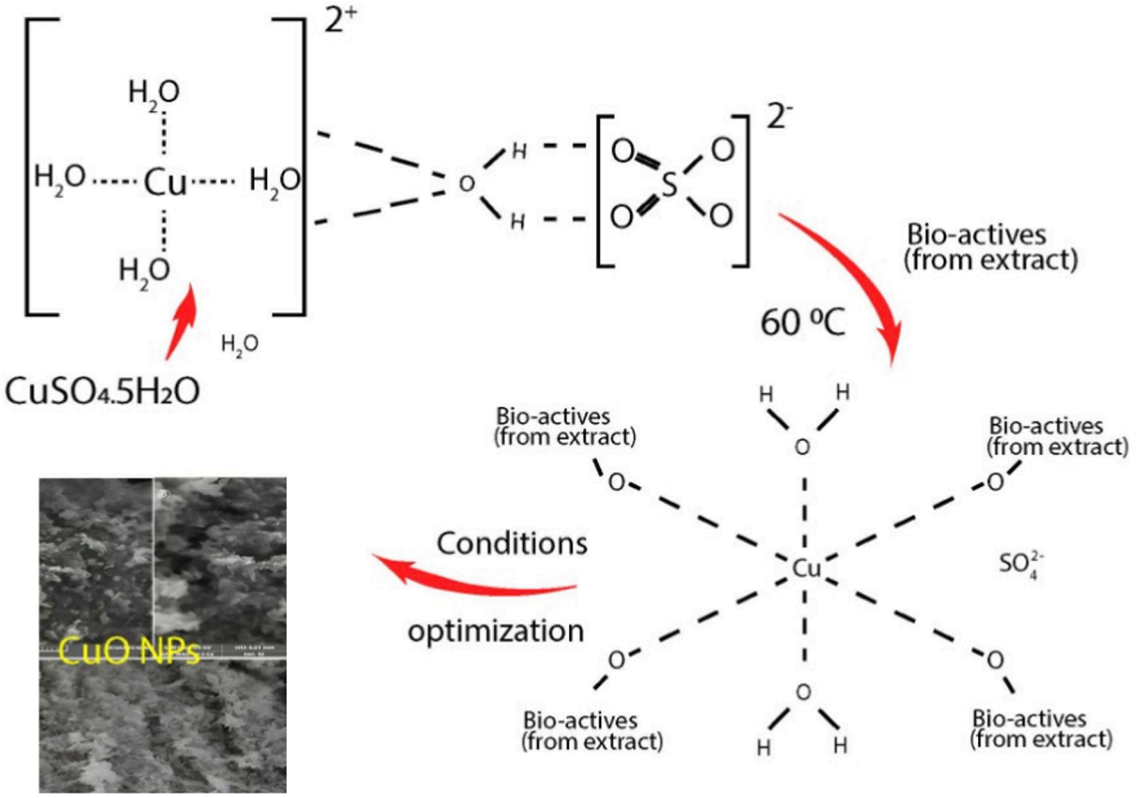

Fig. 1. CuO NPs synthesis mechanism prepared via a green route using *Jasmin sambac* extract. (For interpretation of the references to color in this figure legend, the reader is referred to the web version of this article.)

antifungal agent, poses harm to aquatic life (Iqbal et al., 2019). The environmental impact of MB dye varies based on its application, concentration, and disposal. Caution in use benefits water quality monitoring and medical diagnostics. Improper handling or disposal can result in negative consequences, including water contamination and harm to aquatic life (Ayach et al., 2017, Iqbal et al., 2019).

Effective treatment of textile wastewater, laden with toxic dyes harmful to living organisms, is crucial before discharge. Various methods, such as adsorption, chemical coagulation, membrane separation, photocatalytic degradation, and biological treatment, are employed for addressing water with soluble dyes (Iqbal 2016, Djehaf et al., 2017). Because it removes pollutants and toxins from sewage and industrial effluents, wastewater treatment is critical for environmental and public health protection (Yildirim and Sasmaz 2017). There are various wastewater treatment technologies (Physical, chemical and biological), each with its own set of benefits and drawbacks (Khera et al., 2020, Neolaka et al., 2023). On the other hand, photocatalysis is an effective method for the elimination of toxic dyes from industrial effluents, which destruct the organic pollutants into water, carbon dioxide and inorganic ions (Ali et al., 2021).

The goal of this study was to synthesize CuO NPs from *Jasminium sambac* leaf extract, which is high in flavonoids, phenolics, saponins, and steroids. UV–Vis, SEM, XRD, FTIR, and EDX techniques were used to characterize the samples. This study also examined the influence of process variables on the photocatalytic activity (PCA) in the degradation of Methylene Blue (MB) dye.

2. Experimental

2.1. Reagents and plant samples preparation

Analytical grade chemicals were used in the green synthesis of CuO NPs. Sigma Aldrich provided $CuSO_4{\cdot}5H_2O$ and Methylene Blue, while Merck provided NaOH. The leaves of *Jasminium sambac* (Motia) were collected in Sialkot, Pakistan. Among various extraction techniques (Kusuma and Mahfud, 2017, Kusuma and Mahfud, 2018), the hydro distillation is a method of extraction that is commonly used for the separation of bioactive compounds from plant materials, such as herbs, flowers, or citrus peels. The leaves were washed, dried in the sun, overdried (to a constant weight), and ground to a fine powder. In 100 mL of distilled water, 10 g of powdered leaves were heated at 80 °C with continuous stirring for 15 min. The extract was cooled and filtered, and the supernatant was stored at 4 °C before being used to make CuO NPs.

2.2. Green synthesis of CuO NPs

For CuO NPs synthesis, $CuSO_4{\cdot}5H_2O$ was used as a source of Cu^{+2} ion. 20 mL of 1 M $CuSO_4{\cdot}5H_2O$ was added in 80 mL of plant extract solution, stirred and the color changed to brown suspension, filtered and dried at 60 ^{0}C for 2 h. The following different parameters were optimized for the synthesis of CuO NPs. Salt concentration was optimized by varying the salt concentration from 0.1 to 2 M with constant pH (pH 8), temperature (60 °C), and time (30 min). Optimization of pH was done at different pH (2–8 pH) with constant temperature (60 °C) salt concentration (1 M), and time (30 min). The temperature effect was studied by varying the temperature from 30 to 90 °C at constant time (30 min), pH (pH 8), and salt concentration (1 M). The effect of reaction time was studied in 30–90 min range. The CuO NPs synthesis mechanism prepared via a green route using *Jasmin sambac* extract is depicted in Fig. 1 (Nazir et al., 2023).

Phytochemicals in Jasminum sambac extracts, like alkaloids, flavonoids, tannins, terpenoids, phenolic compounds, saponins, glycosides, and carotenoids, play a vital role in reducing metal ions, contributing to the plant's biological and therapeutic properties. Composition variations stem from factors like plant age, environmental conditions, and extraction methods (Kusuma and Mahfud, 2017, Putri et al., 2019).

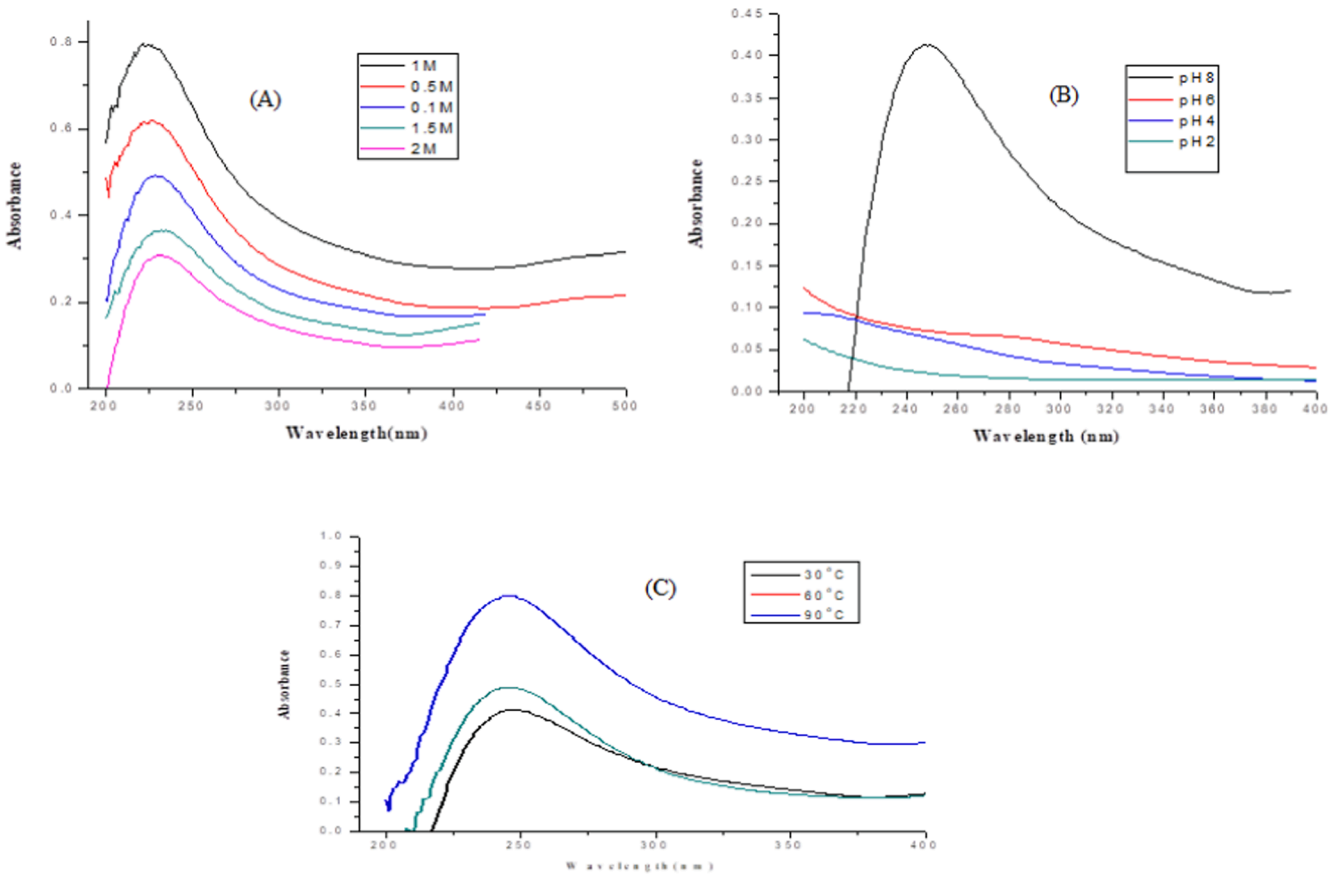

Fig. 2. Effect of process variables on CuO NPs, (A) Effect of concentrations, (B) Effect of pH and (C) Effect of temperatures.

Jasminum sambac extract analysis revealed the identification of 54 bioactive components in the leaf extract. The diverse array of compounds exhibits known biological properties (Tomar and Rijhwani, 2015). The presence of phytochemicals in Jasminum sambac suggests potential health benefits and pharmacological activities, given the well-known diverse biological properties of these compounds (Rattan, 2023). The synthesis of CuO NPs involves the reduction of metal ions, facilitated by the abundance of bioactive compounds in Jasminum sambac. Fig. 1 illustrates the CuO NPs synthesis mechanism using Jasminum sambac extract, following a green route (Nazir et al., 2023). Green synthesis using plant extracts offers advantages like reduced energy consumption, eco-friendly reagents, and scalability, with the mechanism influenced by the bioactive content and chosen extraction technique (Kusuma and Mahfud, 2016, Kusuma and Mahfud, 2017, Kusuma et al., 2018).

2.3. Characterizations

The UV–Visible spectrophotometer was used to measure the wavelength range of 200–800 nm. XRD (Philips PANalytical powder) was used to characterize green synthesized CuO NPs (CuK radiation of wavelength 0.15406 nm in 15 scan range of 20°−80°). To study the morphology, synthesized nanoparticles were examined by using SEM (TESCAN LMU Vega – Variable pressure Scanning Electron Microscope). EDX analysis was performed using an EDX TESCAN LMU Vega to identify elements and determine the chemical composition of elements in synthesized materials, and an FT-IR spectrum was used to identify the reducing and capping agents present in leaf extract and NPs. The Nicolet 6700 FTIR spectrophotometer with a wavelength range of 400 cm^{-1} to 4000 cm^{-1} was used for this analysis.

2.4. Photocatalytic procedure

CuO NPs were used to photocatalyze the degradation of MB dye, which was observed through color change in an aqueous solution exposed to light. After 30 min of stirring in the dark, the CuO NPs and dye mixture reached adsorption–desorption equilibrium before being exposed to light (880.50–890.50 W/m^2 was the intensity of light). A small aliquot of the solution was taken out after a constant interval of time and centrifuged at 3000 rpm for 10 min, before UV visible analysis. Different parameters such as pH (2–12 pH) were analyzed for optimal pH study with constant parameters like time (105 min), concentration of dye (20 ppm), and amount of CuO NPs (50 mg). Optimization study on time (0–120 min) was performed and analyzed with other constant parameters like concentration of dye (50 ppm), amount of CuO NPs (20 mg), and pH 8. The concentration of dye (10–50 ppm) was analyzed for the optimization study with constant parameters like time (90 min) amount of CuO NPs (20 mg) and amount of CuO NPs (10–50 mg) were analyzed for the degradation of MB dye with constant dye concentration (50 ppm), time (120 min), and at pH 8. Percentage photocatalytic degradation was determined using Eq. (1). All the experiments were run in triplicate and data thus obtained was averaged.

$$\text{Photocatalytic degradation}\,(\%) = \frac{(\text{Ao} - \text{At})}{\text{Ao}} \times 100 \quad (1)$$

Where A_o and A_t represent the absorbance values before and after irradiation.

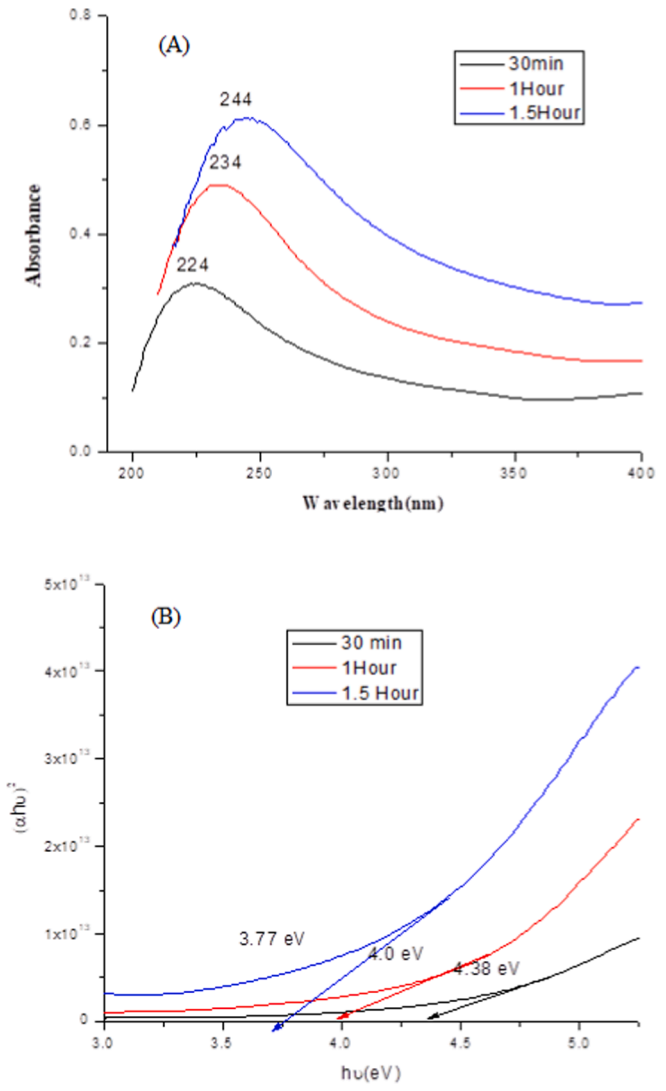

Fig. 3. (A) Effect of reaction time on CuO NPs and (B) Bandgap energy analysis of CuO NPs synthesized by green route. (For interpretation of the references to color in this figure legend, the reader is referred to the web version of this article.)

3. Results and discussion

3.1. Characterization of NPs

3.1.1. Process variables effect on the synthesis of CuO NPs

3.1.1.1. Effect of salt concentration. Fig. 2A represents spectra of CuO NPs at different concentrations of $CuSO_4{\cdot}5H_2O$ (0.1, 0.5, 1, 1.5, and 2 M). At 1 M concentration, maximum absorption was observed at 243 nm. Results showed that the intensity of the absorption decreased with the rise of salt amount from 1 M to 2 M. This may be attributed to the lower concentration of reducing agent and Cu^{+2} ion in higher concentration. Whereas, the minimum value of absorption at 0.1 M concentration may be attributed to the lower concentration of Cu^{+2} ion in the solution. The observations revealed that a salt concentration of 1 M was optimum for the CuO NPs synthesis.

3.1.1.2. Effect of pH. Fig. 2B depicts the pH 2, 4, and 6 effect on the formation of CuO NPs. At alkaline pH (8), an intense spectrum was observed at 243 nm indicating the synthesis of stabilized CuO NPs. Whereas at acidic pH, the reducing and stabilizing agent of plant extract was in their protonated form and therefore, absorption was weak. The results indicate that highly stable, small-sized CuO NPs were synthesized at alkaline pH. Similar results were obtained for NPs synthesis using plant extract, indicating that pH can influence NP formation (Piñero et al., 2017, Kredy 2018).

3.1.1.3. Effect of temperature. Fig. 2C revealed a small shift in absorption peak to longer wavelength with the rise in temperature from 30 °C to 90 °C. This shift is due to the increase in particle size at high temperatures. The SEM image also shows a rise in particle size with temperature. Alike findings have also been reported for the synthesis of NPs using plant extract that the temperature may affect the NPs formation significantly (Kredy 2018).

3.1.1.4. Effect of reaction time. The absorption spectra for CuONP syntheses at 30, 60 and 90 min reaction time are shown in Fig. 3A. The results represent absorption peaks at about 224, 234 and 244 nm, respectively. The small shift in the absorption band at a longer wavelength indicates the increase in particle size. This could be better explained in terms of optical band gap energy, which was determined using Eq. (2).

$$(\alpha h\nu)^n = (h\nu - Eg) \tag{2}$$

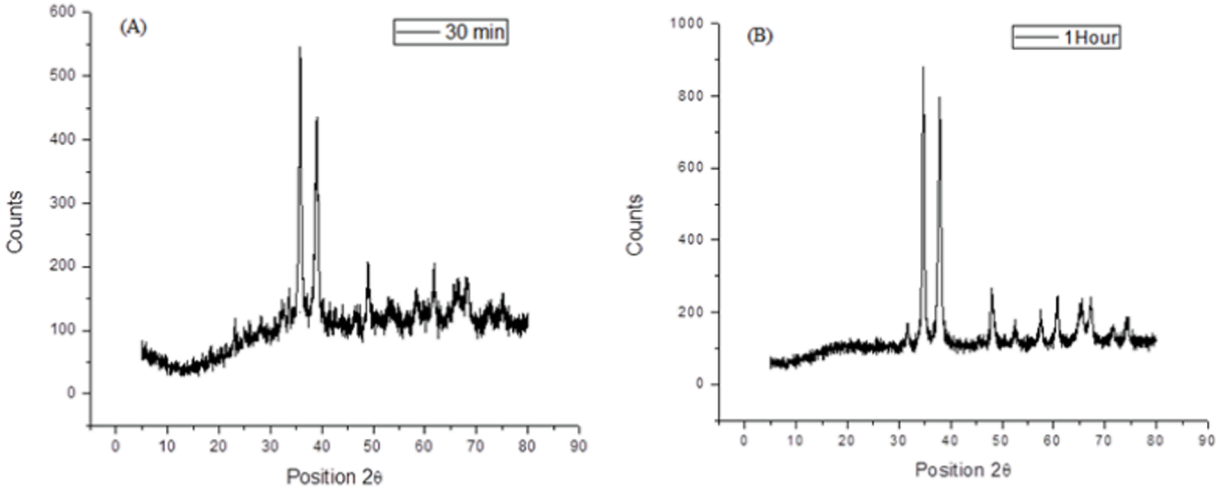

Fig. 4. XRD patterns of CuO NPs at (A) 30 min and (B) 60 min reaction time.

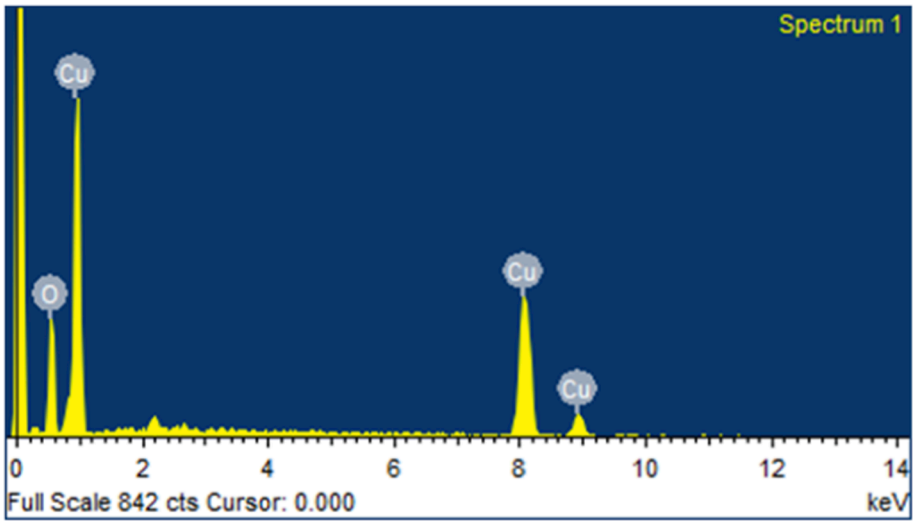

Fig. 5. EDX analysis of CuO NPs synthesized by green route. (For interpretation of the references to color in this figure legend, the reader is referred to the web version of this article.)

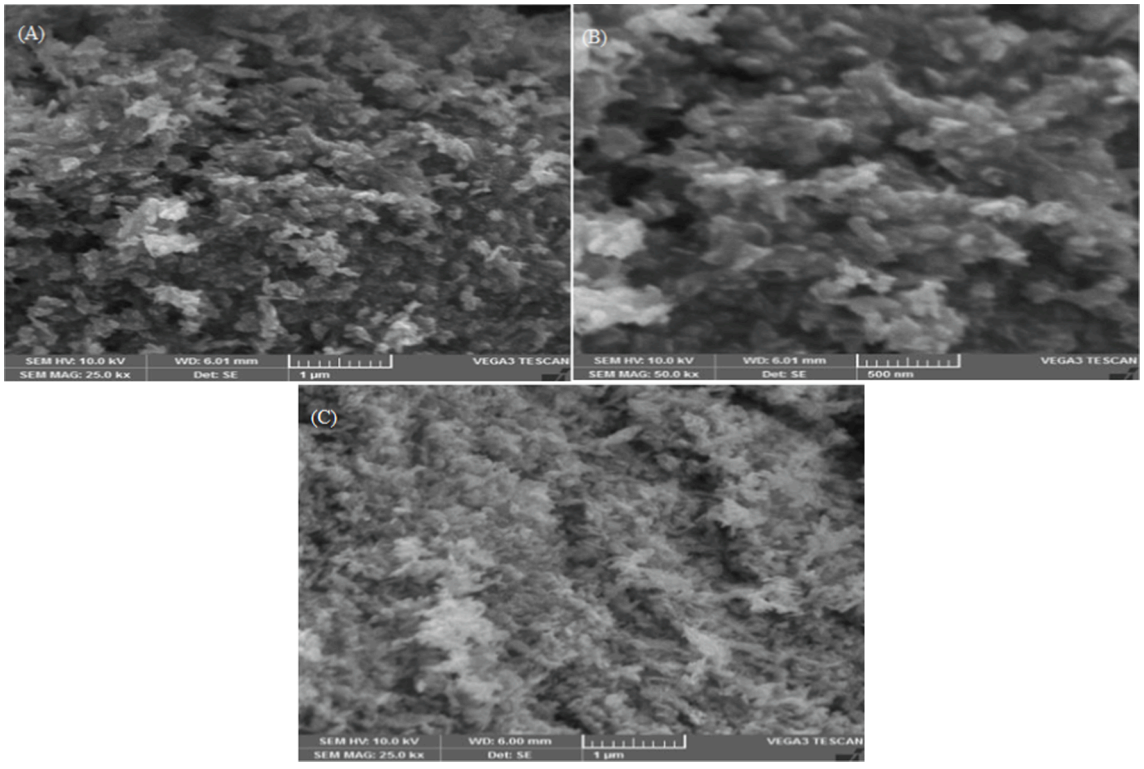

Fig. 6. SEM images of CuO NPs prepared at **(A)** 30 °C, **(B)** 60 °C and **(C)** 90 °C.

Where B is a constant, hv is photon energy in eV, h is planks constant, is photon frequency, Eg is optical band gap energy in eV, n is an exponent transition, and is absorption coefficient. The increase in reaction time is responsible for the shift in band gap energy (Fig. 3B). As the particle size decreases to the nanoscale, the energy level decreases and electron becomes more confined in the particles. This increases the band gap energy between the valance and conduction bands. This explains why NPs have a higher band gap energy than comparable large-size materials. (Naseer et al., 2020). Furthermore, the XRD analysis results show that the CuO NPs size increases with reaction time, from 13.4 to 15.7 nm.

3.2. XRD analysis

The CuO NPs formation was confirmed by XRD analysis (Philips PANalytical powder) using CuKα radiation of wavelength 0.15406 nm in a scan range of 20°-80°. X-ray diffraction pattern show (Fig. 4) showed sharp peaks at 35.71°, 38.93°, 48.98° and 62.07°, indicating the formation of the CuO NPs monoclinic and crystalline in nature. The size (D) of CuO NPs obtained by using applying the Debye-Scherrer formula (Eq. (3) was found 13.4 nm.

$$D = \frac{0.9\lambda}{\beta \cos\theta} \tag{3}$$

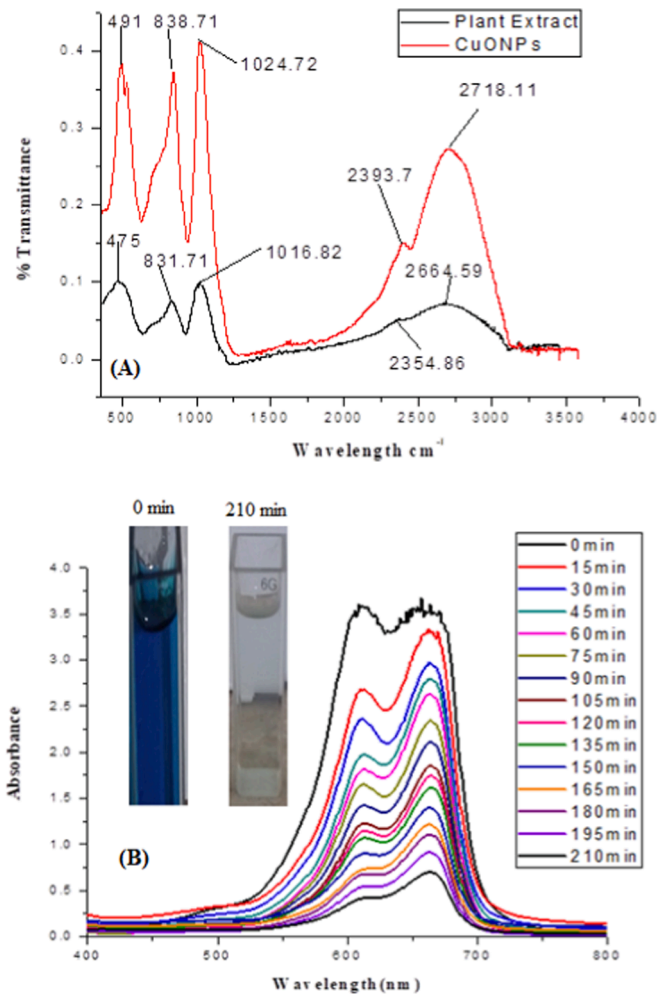

Fig. 7. (A) FTIR analysis of leaf extract of *Jasminium sambac* and CuO NPs and (B) UV–visible analysis of Methylene Blue dye untreated and treated up to 120 min. (For interpretation of the references to color in this figure legend, the reader is referred to the web version of this article.)

The X-ray diffraction patterns of CuO NPs prepared using *Jasminium sambac* leaves extract are closely related to the XRD pattern of CuO NPs previously reported (Das et al., 2013). Also, (Acharyulu et al., 2014, Shi et al., 2017) reported pure crystallite and well-defined CuO NPs using *C. auriculata* and *P. amarus* leaf extract, respectively.

3.3. EDX and SEM analysis

The elemental composition of CuO NPs was validated using energy dispersive X-ray analysis (EDX). The EDX analysis confirms the presence of Cu and O elements, as shown in Fig. 5, with percentages of 75.94 and 24.06, respectively. CuO NPs exhibit a strong diffraction band peak at 1 keV, which is typical of copper absorption due to surface plasmon resonance. SEM was used to examine the morphology of green fabricated CuO NPs, and the results are shown in Fig. 6. The average size of CuO NPs was discovered to be consistent with XRD analysis. Because of the interaction between biomolecules capping the individual particle, the CuO NPs had irregular shapes and aggregated.

3.4. FTIR analysis

FT-IR analysis is employed for the identification of functional groups (Syafaatullah and Mahfud 2021), which is used to identify the bioactives in the leaf extract of *Jasminium sambac*. It is also used to study the effective incorporation of phytochemicals in the synthesis of CuO NPs. FTIR spectrum (Fig. 7A) of CuO NPs and leaf extract was recorded in the 400 to 4000 cm^{-1} range. The band at 2718.11 cm^{-1} is ascribed to C–H vibration. While a band at 1024.72 cm^{-1} and 831.71 cm^{-1} are associated with C–N stretching in primary amine and C–C vibrations in the alkyl group present in plant extract. The bands at 2354.86 cm^{-1} show the alkyne C≡C stretching vibration, which indicates the presence of lipid molecules in the leaf extract. The most significant absorption band detected at 491 cm^{-1} is allocated to metal–oxygen vibration (Shi et al., 2017).

3.5. Photocatalytic activity of CuO NPs

3.5.1. Effect of pH

The impact of solution pH on dye degradation was investigated by varying pH levels from 2 to 12. Experiments were conducted with a fixed dye concentration of 20 ppm and 50 mg of CuO NPs. The degradation efficiency of CuO NPs was found to be 52.63, 61.1, 69.51, and 79.82 (%), at pH 2, 4, 6, 8, and 12, respectively (Table 1). In alkaline pH, a negative charge is induced on the CuONP surface and enhances the formation of reactive species that effectively degrade the cationic dye. At acidic pH, there were no significant electrostatic attractions between the CuONP surface and MB dye molecules. Therefore, the extent of photocatalytic degradation of MB dye was decreased at acidic pH. It is evident from the results that, an increase in pH from 2 to 8 accelerates photocatalytic degradation, while at pH 12, the photocatalytic degradation efficiency of CuO NPs declined. The reason is attributed to the excess of anions formation at pH > 8 (Acharyulu et al., 2014). Anions compete with dye molecules to adsorb on CuONP surface active sites, hindering adsorption and reducing photocatalytic degradation of MB dye. At pH_{pzc} is the point where nanoparticles surface charge became neutral. CuO nanoparticles have an amphoteric behavior, which means they can be positively or negatively charged depending on the pH of their surroundings. Understanding the nature of the binding active site on the surface of CuO nanoparticles requires an understanding of the point of zero charge (pH_{pzc}). (Noreen et al., 2020). For this, a various solution of CuO nanoparticles were prepared in NaCl solution and then, their initial pH was adjusted using NaOH/HCl solutions and final pH values were estimated after 24 h. The pH < pH_{pzc} favors the adsorption of cationic species, while pH < pH_{pzc} favors anionic species adsorption. The pH data thus obtained was used to measure the change in pH values and a plot was drawn between initial pH and ΔpH (pH_i-pH_f) The data revealed that the values of pH_{pzc} of CuO nanoparticles was 6.27. The pH_{pzc} data revealed that the CuO nanoparticle bear positive charge and negative above the pH_{pzc}. Also, the findings of present investigation support these observations. In basic pH, the dye degradation was higher, which is due to the negative charge on the surface of CuONP surface that enhances the reactive species formation (Liang et al., 2017). The cationic dye was effectively attracted to the CuONP surface, enhancing dye removal through the oxidative process, particularly in basic media.

3.5.2. Effect of CuO NP dose

The dose of CuO NPs has a substantial influence on dye destruction. The photocatalytic degradation of dye was increased by increasing the amount of catalyst. As the concentration of CuO NPs increased from 10 mg to 50 mg, the degradation efficiency of MB dye increased from 11.62% to 80.67% (Table S1). This phenomenon is due to the augmentation of active sites on the catalyst, which results in optimal adsorption of dye molecules onto the catalyst's surface and the generation of additional reactive species for dye degradation.

3.5.3. Effect of dye initial concentration

The effect of the concentration of MB dye on photocatalytic degradation was investigated in 10 to 50 mg/L. By enhancing the dye concentration, the dye removal was declined (Table S2). This might be due to the obstruction in the path of incident light due to the increased

Table 1
Effect of medium pH on the MB dye degradation using CuO NPs.

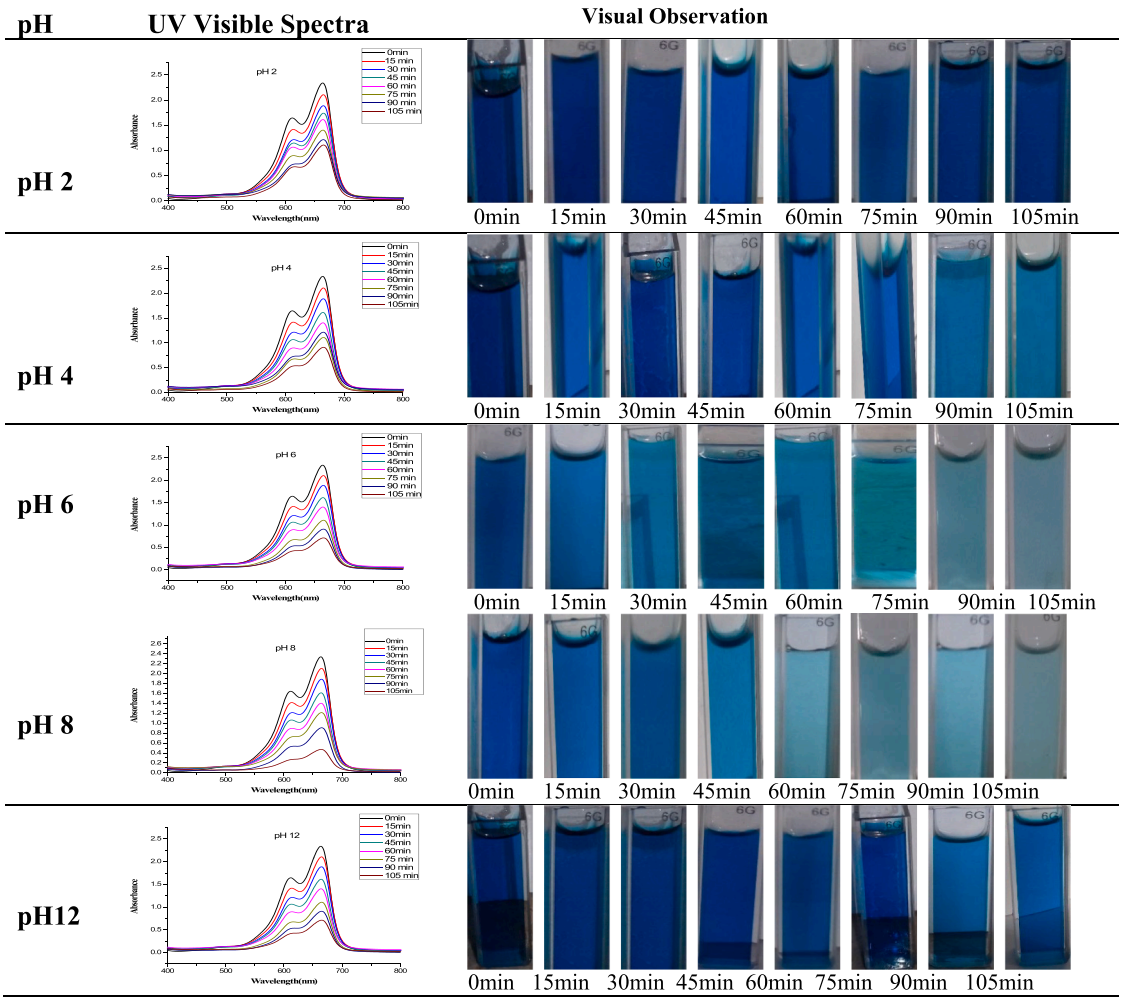

concentration of dye, which precludes the light from reaching the catalyst surface, thus leading to a decrease in degradation efficiency. Secondly, the adsorption of MB molecules on the catalyst surface suppressed the generation of reactive species, and resultantly, degradation efficiency was decreased.

3.5.4. *Effect of contact time*

The impact of contact time on photocatalytic degradation is shown in Fig. 7B. The before irradiation of catalysts and dye mixture to the light, the catalysts and dye mixture was stirred in dark for 30 min to check to attain the adsorption–desorption mechanism of dye. Before irradiation to light, 3 mL dye sample was taken and its absorbance was monitored. It was observed that 1.72% dye was adsorbed during the adsorption–desorption equilibrium attainment and this value was considered the initial concentration of dye. After irradiation, the MB dye degradation was 47.21% at the first 15 min of irradiation, which increased gradually and reached 97.67% after 210 min of irradiation. The initial sharp increase in dye degradation results from dye adsorption. Over time, degradation products compete with dye ions for adsorption on the catalyst surface, slowing down the photocatalytic degradation process. The kinetics of MB dye degradation, assessed through first-order and second-order models, are depicted in Figs. S1-S3. Photocatalytic dye degradation is significantly influenced by catalyst surface adsorption and subsequent degradation by reactive species. The MB dye degradation follows pseudo-first-order kinetics (Fig. S2). The mechanism of MB dye degradation under light irradiation using CuO NPs is shown in Eqs. 4–8. The electrons excitation from VB to CB produces an e^- and h^+ pair upon irradiation. The e^- (CB) reacts with O_2 and give a superoxide radical, while the h^+ reacts with H_2O to form $^{\bullet}OH$ radical. The $^{\bullet}OH$ radicals are reactive species that degrade the MO dye oxidatively into a low molecular weight intermediate and, finally, into H_2O, CO_2, and inorganic ions (Eqs. 4–8). The proposed MB dye degradation mechanism using CuO NPs prepared via green route is depicted in Fig. 8. PCA of CuO NPs shows potential for cost-effective MO dye removal under light, offering an economical solution for MB dye remediation, which is also in line with previous studies (Table 2). Green synthesis, using natural compounds like plant extracts, microorganisms, and green reducing agents, is an eco-friendly approach with catalytic applications. Consideration of plant extract and extraction method is crucial for tailoring nanoparticles to specific properties and applications (Sinha and Ahmaruzzaman 2015, Wang et al., 2019, Kusuma et al., 2023).

$$NPs + \text{irradiation} \rightarrow NPs\,(VB)h^+ + (CB)e^- \quad (4)$$

$$H_2O + h^+ \rightarrow {}^{\cdot}OH + H^+ \quad (5)$$

$$e^- + O_2 \rightarrow O_2^{-\bullet} \quad (6)$$

$$2H^+ + O_2^- \rightarrow HO_2^- + H^+ \rightarrow 2OH^{\cdot} \quad (7)$$

$$\text{MB dye} + {}^{\bullet}OH \rightarrow H_2O_2 + CO_2 + \text{inorganic ions} \quad (8)$$

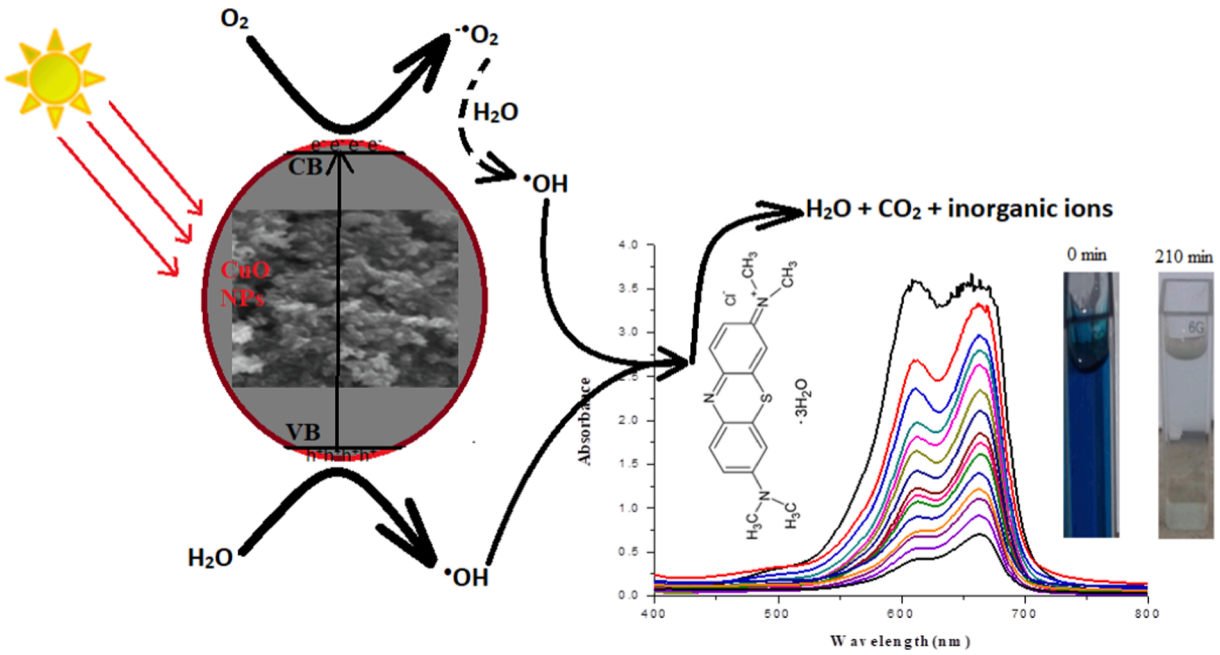

Fig. 8. The proposed MB dye degradation mechanism using CuO NPs prepared via green route. (For interpretation of the references to color in this figure legend, the reader is referred to the web version of this article.)

Table 2
A comparison of synthesis route, properties and application of Cu and CuO NPs.

Sr. #	NPs	Source material/methods	Results	Applications	References
1	Cu	Extract fish scales of *Labeo rohita*	size = 25–37 nm, λ = 589 nm, monodispersed, spherical	Active catalytic	(Sinha and Ahmaruzzaman 2015)
2	Cu	Electrolytic deposition $CuSO_4$ solution	Irregular shape, agglomerated, size = 40 nm	Antimicrobial, Photovoltaic	(Wang et al., 2019)
3	CuO	Green synthesis using Bougainvillea flowers extract	Highly stable, spherical in shape and diameter = 12 ± 4 nm, λ = 274 nm	Active antifungal	(Shammout and Awwad 2021)
4	CuO	Thermal decomposition methods	λ = 380 nm, spherical, particle size = 15–30 nm,	Antioxidant, antibacterial	(Das et al., 2013)
5	CuO	Green synthesis using Cassia auriculata leaf extract	Monoclinic, λ = 285 nm, spherical, particle size = 22.4 nm	Biocompatible towards RAW 264.7 cell lines	(Shi et al., 2017)
	CuO	Green synthesis using *Jasmin sambac* extract	Monoclinic, λ = 243, particle size = 13.4 nm, irregular shapes, in aggregate form	Photocatalytic activity	Present study

3.6. Reusability and recyclability of the catalyst

The development of green technologies is a key focus in industrial discharged water treatment strategies, with a focus on the repeated use of photocatalysts because of their advantages in terms of both cost and environmental impact. The reusability of the catalyst is assessed over the course of six cycles. The CuONP was separated from the reaction mixture of MB dye degradation, washed with distilled water, and dried before being added to a new dye solution for further cycles of photodegradation in order to evaluate its reusability. MB degradation was 97.67% in the first cycle, declined slightly to 96.1% in the second cycle, and showed 94.6% degradation in the third cycle. In the sixth cycle, the MB dye degradation decreased even more, reaching 89.9% (Fig. S4). The decline in catalytic activity is attributed to dye accumulation on active sites. Reusable catalysts in photocatalytic processes offer environmental and economic sustainability by reducing resource consumption, waste, and overall environmental impact. Single-use catalysts, especially those with hazardous or difficult-to-recycle components, pose disposal challenges, making reusability a more sustainable choice.

4. Conclusion

The synthesis of copper oxide nanoparticles (CuO NPs) utilized Jasminum sambac leaf extract, wherein nanoparticle characteristics were notably influenced by solution pH, temperature, reaction time, and copper sulfate concentration. The resulting CuO NPs were monodisperse, crystalline, monoclinic, and exhibited purity, with a particle size of 13.4 nm. These NPs displayed promising photocatalytic activity, achieving a notable 97% removal of Methylene Blue (MB) dye after 210 min of light exposure. Factors such as pH, CuO NPs dosage, and MB dye concentration influenced the photocatalytic performance. The green synthesis method using Jasminum sambac leaf extract proves highly efficient for tailoring CuO NPs for photocatalytic applications. Future research will focus on evaluating photocatalytic activity under visible light and studying the toxicity of treated MB dye, including the identification of intermediate byproducts.

Declaration of Competing Interest

The authors declare that they have no known competing financial interests or personal relationships that could have appeared to influence the work reported in this paper.

Acknowledgements

The authors express their gratitude to Princess Nourah bint Abdulrahman University Researchers Supporting Project number (PNURSP2024R11), Princess Nourah bint Abdulrahman University, Riyadh, Saudi Arabia. We are thankful to anonymous reviewers for their valuable suggestions for the improvement of the article contents.

Appendix A. Supplementary data

Supplementary data to this article can be found online at https://doi.org/10.1016/j.jksus.2024.103089.

References

Acharyulu, N., Dubey, R., Swaminadham, V., et al., 2014. Green Synthesis of CuO Nanoparticles using Phyllanthus Amarus Leaf Extract and theirAntibacterial Activity Against MultidrugResistance Bacteria. Int. J. Eng. Res. Technol. 3 (4), 639–641.

Alfanaar, R., Elim, P.E., Yuniati, Y., et al., 2021. Synthesis of TiO2/ZnO-anthocyanin hybrid material for dye sensitized solar cell (DSSC). IOP Conference Series: Materials Science and Engineering. IOP Publishing.

Ali, F., Hamza, M., Iqbal, M., et al., 2021. State-of-art of silver and gold nanoparticles synthesis routes, characterization and applications: a review. Zeitschrift für Physikalische Chemie. 236 (3), 291–326.

Amer, M.W., Awwad, A.M., 2021. Green synthesis of copper nanoparticles by *Citrus limon* fruits extract, characterization and antibacterial activity. Chem. Int. 7 (1), 1–8.

Ayach, A., Fakhi, S., Faiz, Z., et al., 2017. Adsorption of methylene blue on bituminous schists from Tarfaya-Boujdour. Chem. Int. 3 (4), 442–451.

Das, D., Nath, B.C., Phukon, P., et al., 2013. Synthesis and evaluation of antioxidant and antibacterial behavior of CuO nanoparticles. Colloids Surfaces B: Biointerfaces 101, 430–433.

Djehaf, K., Bouyakoub, A.Z., Ouhib, R., et al., 2017. Textile wastewater in Tlemcen (Western Algeria): Impact, treatment by combined process. Chem. Int. 3 (4), 414–419.

Iqbal, M., 2016. Vicia faba bioassay for environmental toxicity monitoring: A review. Chemosphere 144, 785–802.

Iqbal, M., Abbas, M., Nazir, A., et al., 2019. Bioassays based on higher plants as excellent dosimeters for ecotoxicity monitoring: A review. Chem. Int. 5 (1), 1–80.

Khera, R.A., Iqbal, M., Ahmad, A., et al., 2020. Kinetics and equilibrium studies of copper, zinc, and nickel ions adsorptive removal on to Archontophoenix alexandrae: conditions optimization by RSM. Desalination Water Treatment. 201, 289–300.

Kredy, H.M., 2018. The effect of pH, temperature on the green synthesis and biochemical activities of silver nanoparticles from Lawsonia inermis extract. J. Pharm. Sci. Res. 10 (8), 2022–2026.

Kusuma, H., Mahfud, M., 2016. Response surface methodology for optimization studies of microwave-assisted extraction of sandalwood oil. J. Mater. Environ. Sci. 7 (6), 1958–1971.

Kusuma, H.S., Lestari, F.W., Sari, T.A., et al., 2023. Extraction of essential oil from fresh basil leaves (Ocimum basilicum L.) using solvent-free microwave extraction method: Extraction parameter optimization, electric consumption, and CO2 emission study. Food and Humanity. 1, 1055–1063.

Kusuma, H.S., Mahfud, M., 2018. Kinetic studies on extraction of essential oil from sandalwood (Santalum album) by microwave air-hydrodistillation method. Alex. Eng. J. 57 (2), 1163–1172.

Kusuma, H.S., Altway, A., Mahfud, M., 2018. Solvent-free microwave extraction of essential oil from dried patchouli (Pogostemon cablin Benth) leaves. J. Ind. Eng. Chem. 58, 343–348.

Liang, Y., Chen, Z., Yao, W., et al., 2017. Decorating of Ag and CuO on Cu nanoparticles for enhanced high catalytic activity to the degradation of organic pollutants. Langmuir 33 (31), 7606–7614.

Nagesh, M.R., Kumar, N., Khan, J.M., et al., 2022. Green synthesis and pharmacological applications of silver nanoparticles using ethanolic extract of Salacia chinensis L. J. King Saud Univ. - Sci. 34 (7), 102284.

Naseer, A., Ali, A., Ali, S., et al., 2020. Biogenic and eco-benign synthesis of platinum nanoparticles (Pt NPs) using plants aqueous extracts and biological derivatives: environmental, biological and catalytic applications. J. Mater. Res. Technol. 9 (4), 9093–9107.

Nazir, A., Alam, S., Alwadai, N., et al., 2023. Green synthesis of copper nanoparticles using Citrullus colocynthis leaves extract: photocatalytic, antimicrobial and antioxidant studies. Zeitschrift für Physikalische Chemie. 237 (11), 1733–1751.

Neolaka, Y.A.B., Lawa, Y., Naat, J., et al., 2023. Adsorption of methyl red from aqueous solution using Bali cow bones (Bos javanicus domesticus) hydrochar powder. Results Eng. 17, 100824.

Noreen, S., Khalid, U., Ibrahim, S.M., et al., 2020. ZnO, MgO and FeO adsorption efficiencies for direct sky Blue dye: equilibrium, kinetics and thermodynamics studies. J. Mater. Res. Technol. 9, 5881–5893.

Piñero, S., Camero, S., Blanco, S., 2017. Silver nanoparticles: Influence of the temperature synthesis on the particles' morphology. Journal of Physics: Conference Series, IOP Publishing.

Putri, D.K.Y., Dewi, I.E.P., Kusuma, H.S., et al., 2019. Extraction of an essential oil from fresh cananga flowers (Cananga odorata) using solvent-free microwave method. J. Chem. Technol. Metall. 54 (4), 793–802.

Rattan, R., 2023. Bioactive phytochemicals from Jasminum species. J. Emerg. Technol. Innovat. Res. 10 (5), 198–203.

Shammout, M.W., Awwad, A.M., 2021. A novel route for the synthesis of copper oxide nanoparticles using Bougainvillea plant flowers extract and antifungal activity evaluation. Chem. Int. 7 (1), 71–78.

Shi, L.-B., Tang, P.-F., Zhang, W., et al., 2017. Green synthesis of CuO nanoparticles using Cassia auriculata leaf extract and in vitro evaluation of their biocompatibility with rheumatoid arthritis macrophages (RAW 264.7). Trop. J. Pharm. Res. 16 (1), 185–192.

Sinha, T., Ahmaruzzaman, M., 2015. Green synthesis of copper nanoparticles for the efficient removal (degradation) of dye from aqueous phase. Environ. Sci. Pollut. Res. 22 (24), 20092–20100.

Sivakavinesan, M., Vanaja, M., Lateef, R., et al., 2022. Citrus limetta Risso peel mediated green synthesis of gold nanoparticles and its antioxidant and catalytic activity. J. King Saud Univ. - Sci. 34 (7), 102235.

Syafaatullah, A. Q. and M. Mahfud, 2021. Optimization extraction of Indigofera tinctoria L. using microwave-assisted extraction. IOP Conference Series: Materials Science and Engineering, IOP Publishing.

Tomar, K., Rijhwani, S., 2015. Evaluation of antibacterial activity of Phytoconstituents isolated from Jasminum sambac L. and their identification through GC-MS. International Journal of Engineering Technology, Management. Appl. Sci. 215 (3), 451–459.

Wang, L., Gopinath, S.C., Anbu, P., et al., 2019. Photovoltaic and antimicrobial potentials of electrodeposited copper nanoparticle. Biochem. Eng. J. 142, 97–104.

Widowati, W., Janeva, W., Nadya, S., et al., 2018. Antioxidant and antiaging activities of Jasminum sambac extract, and its compounds. J. Rep. Pharm. Sci. 7 (3), 270–285.

Yildirim, D., Sasmaz, A., 2017. Phytoremediation of As, Ag, and Pb in contaminated soils using terrestrial plants grown on Gumuskoy mining area (Kutahya Turkey). J. Geochem. Explor. 182, 228–234.